Short-Term Failure Warning for Transmission Tower Under Land Subsidence Condition

LI ZHANG[1], JIANGJUN RUAN[1], (Member, IEEE), ZHIYE DU[1], (Member, IEEE), WENFENG ZHOU[1], GUANNAN LI[1], AND YAN GAN[2]

[1]School of Electrical Engineering and Automation, Wuhan University, Wuhan 430072, China
[2]Central China Branch of State Grid Corporation of China, Wuhan 430072, China

Corresponding author: Li Zhang (zhangliwhu@whu.edu.cn)

ABSTRACT Crustal movement and land subsidence will cause tower foundation settlement, which seriously affects the safety of transmission line operation. This paper proposed a short-term failure warning method for transmission tower under land subsidence condition based on finite element method, strain monitoring and time series prediction. By simulating the stress distribution of the tower in actual foundation settlement, the weak components of the settlement tower were founded. Combined with the finite element simulation results in various conditions, the reliability of simulation results is verified, and the strain variation range of the corresponding measuring point is obtained. By installing the real-time strain monitoring system and establishing the autoregressive integrated moving average (ARIMA) time series forecast model, warning of the failure of the tower can be sounded in short time according to the strain monitoring and forecasting results. The field results show that the tower is in good condition and with no risk in short term. The method proposed by this paper is economical and easy to operate, which can be used to conduct the emergency treatment of the dangerous tower under land subsidence condition.

I. INTRODUCTION

Transmission line is the key facility of power grid system all over the world. According to statistics, natural disasters are the primary cause of transmission tower damage [1]. High voltage transmission lines are usually of several hundred kilometers long and may pass through complex topography or seismically active zones. Research shows that in many mountainous areas and hilly areas, crustal movement and land subsidence will lead to tower foundation settlement, which may further cause the yield of steel structure or even collapse of transmission towers. It will seriously affect the safety of transmission line operation. But the existing approaches cannot accurately monitor the safety margin of tower, which brings great inconvenience to grid corporations. This paper aims to address such challenge by accurately monitoring and judging safety of transmission line tower in real time, so that the State Grid Corporation can make correct emergency decisions [2]–[4].

In recent years, the failure mechanism of transmission towers under icing and wind loads had been systematically

studied based on the finite element model in mechanical simulation of tower, while few have studied the mechanical characteristics of towers under foundation settlement [5]–[10]. The tower-line system finite element modeling has become a general analysis method to study the tower failure problem. Huang *et al.* [3] analyzed the variation law of the maximum equivalent stress undertaken by the components of tower for different tower foundation settlement conditions. Du *et al.* [7] used beam element and cable element to establish the integral finite element model of towers, lines and insulators, and analyzed the mechanical properties and weak steel structure for towers in specific ice-coated microclimate zone.

At present, some online monitoring devices have been installed in the tower to evaluate its status. Existing real-time monitoring methods of tower are as follows: inclination monitoring based on tilt sensor [11], [12], deformation monitoring based on satellite technology [13], strain monitoring based on resistance strain sensor and strain monitoring based on optical fiber sensor, etc. The first two can replace traditional manual inspection, but they can only reflect the overall load and load balance state of the tower indirectly. Partial failure of tower and advanced warning of tower damage can't be realized [14]. Resistance strain sensor is low-cost and convenient to install,
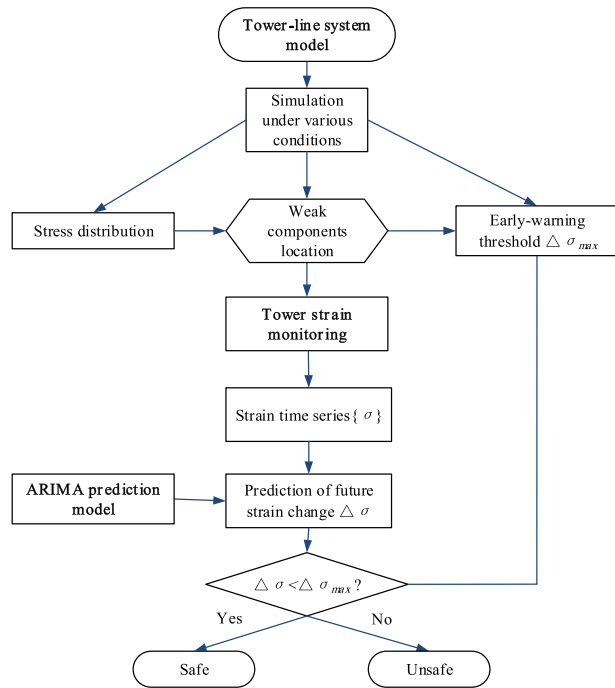
The associate editor coordinating the review of this manuscript and approving it for publication was Hao Luo.

FIGURE 1. Flowchart of short-term tower failure warning method.

FIGURE 2. Site photos. (a) Photos of the foundation, (b) Photos of the deformed steels.

but it is too easily damaged by the harsh environment to be suitable for long-term online monitoring. Fiber Bragg grating (FBG) sensors have the advantages of corrosion resistance, anti-electromagnetic interference and high sensitivity, but it's expensive and difficult to install [14]–[17].

Thus, how to combine simulation results with actual measurement of transmission tower to give early warning of tower instability entails further study, and there are few researches on the future condition prediction of towers.

This paper, taking a 500kV transmission line as an example, puts forward a short-term failure warning method for transmission tower under land subsidence condition, which is shown in Fig.1. Combined with the finite element simulation results, angle iron strain monitoring and time series forecast model based on ARIMA, warning of failure of the tower can be sounded in short time, which can be utilized to conduct emergency treatment of the dangerous towers under land subsidence condition. The method is low-cost and easy to operate, and it is of great significance to the safe and stable operation of power grid.

II. TOWER-LINE SYSTEM FINITE ELEMENT MODEL
A. SITE CONDITIONS
In Hubei Province, China, the staff of State Grid Corporation found some deformed members of a 500kV transmission tower and obvious cracks between the foundation and the protecting surface, signifying a high probability of failure which may affect the safe operation of the power grid. According to experts' analysis, geological collapse, landslide and karst ground collapse occurred in this area. The soil 10 meters below the ground has been creeping for a long time, which
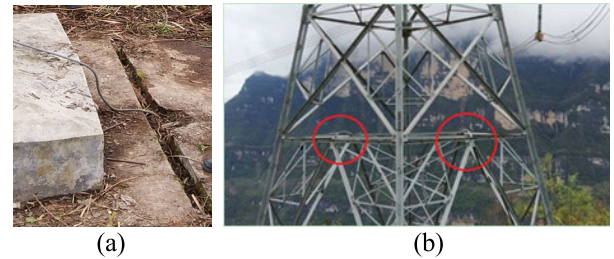
caused tower foundation deformation and turbulent distribution of forces on the tower steels. Steels located on the first transverse partition of the tower are bent upward. Site photos of the settled foundation and deformed steels have been shown in Fig.2.

The tower is an angle tower. Its number is 18#. Its type is SJ3A-24 and angle of rotation is 30° 44. The tension section where the tower is located consists of 11 towers. The main elements and auxiliary elements of the tower are made of Q345 steel and Q235 steel. The type of the conductors and the ground wires is LGJ-630/55 and GJ-80.

Considering that the tower has a high probability of mechanical failure, a new tower is needed to replace it. But the condition of the tower 18# needs to be monitored before a new tower is built so that workers can make timely response and reduce possible losses caused by tower failure.

B. FINITE-ELEMENT MODEL
Mechanical simulation study of the tension section composed of towers, conductors and ground wires is carried out, finite element mechanical model of tension section is established, and stress distribution of each steel structure on tower is analyzed. The general FEA software ANSYS is applied for the tower structural analysis. It has a wide range of applications in the field of structural mechanics calculation. For mechanics analysis of transmission tower-line system, it has a great advantages in modeling, loading, solving algorithms and post-processing. The members of the towers are simulated by the BEAM188 element, which is a uniaxial element with tension, compression, torsion, and bending capabilities. The real constant of BEAM 188 element is set to simulate the shape and section size of L-shaped angle steel. The conductors and the ground wires are simulated by the LINK10 element with nonlinear, stress hardening and large deformation function. LINK8 rigid link element is used to simulate insulator string. Then a 1:1 refined solution model of 3d finite element can be established. The establishment of the model is completely consistent with the actual system.

Under normal circumstances, the conductors and ground wires of overhead transmission lines are of catenary structures under the action of gravity with a balance of various forces to simplify the model, the 6 split wire is equivalent to a single wire. After equivalence, the initial strain, weight of the unit length line and tension should be ensured to be the same
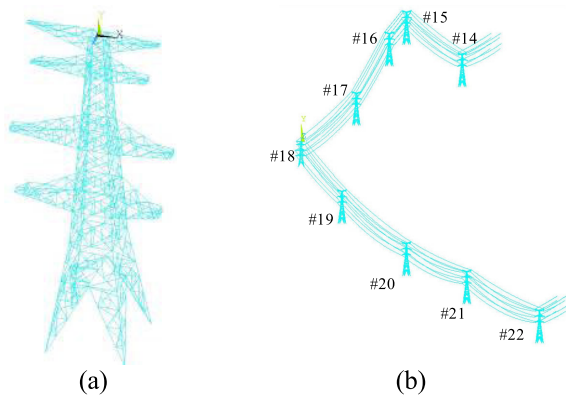
FIGURE 3. Finite element model. (a) Simulation model of tower 18#, (b) Simulation model of the whole strain section.

FIGURE 4. Schematic diagram of tower 18# leg displacement.

as that of a single conductor. The equivalent diameter d_{eq} is calculated according to the following equation:

$$d_{eq} = D(Sd/D)^{1/s} \qquad (1)$$

where S is splitting number of the conductor, D is diameter of each divided conductor; d is diameter of the conductor.

The suspended line equation of conductors is as follows:

$$\begin{cases} y = \dfrac{\sigma_0 h}{\gamma L_{h=0}}(\sinh \dfrac{\gamma l}{2\sigma_0} + \sinh \dfrac{\gamma(2x-l)}{2\sigma_0}) \\ -(\dfrac{2\sigma_0}{\gamma}\sinh \dfrac{\gamma x}{2\sigma_0} \sinh \dfrac{\gamma(l-x)}{2\sigma_0})\sqrt{1+(\dfrac{h}{L_{h=0}})^2} \\ L_{h=0} = \dfrac{2\sigma_0}{\gamma}\sinh \dfrac{\gamma l}{2\sigma_0} \end{cases} \qquad (2)$$

where l is the horizontal distance between two suspension points of conductors, h is the vertical distance between two suspension points of conductors; γ is the ratio of the gravity per unit length of the conductor to its section; σ_0 is the stress at the lowest point of the conductor.

Integrated tower-line system simulation model of the whole strain section is shown in Fig.3.

C. BOUNDARY CONDITIONS

The main components of transmission tower-line system include towers, conductors, ground wires and insulator strings. In addition to the inherent loads the tower-line system sustained, due to the settlement of the tower foundation, the tower leg joints have deviated from its original position. So it is needed to apply nonzero displacement constraints to the tower leg joints whose position has changed. On account of the weather and geographical location of the transmission tower-line system, there was little wind and ice covered on the surface of lines, so that the additional loads, such as ice load or wind load, borne by the tower-line system is not considered in this paper.

Considering the stress field of towers and wires caused by gravity field, set material density and gravity acceleration to simulate gravity effects in ANSYS,the standard gravity acceleration 9.8m/s^2 is adopted in this paper.
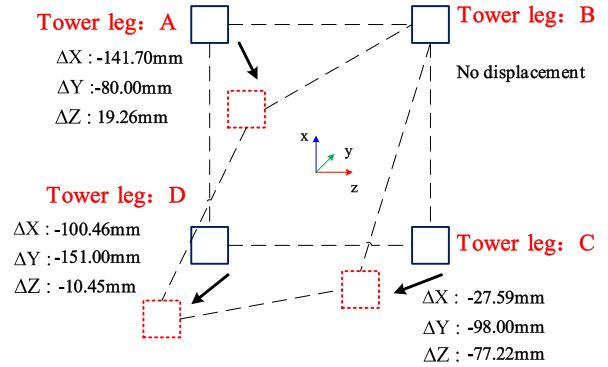
As a result of tower foundation settlement, the position of several tower legs has been significantly changed. However, according to recent monitoring data, the position of tower legs is basically stable in short term and the changes are extremely slow. Therefore, it is assumed that the displacement of connection points of the tower legs and foundation of tower #18 will not change in the static finite element simulation. A nonzero displacement constraint in the direction of movement is applied to the connecting points of the tower legs whose positions have changed,and zero displacement constraint in the other direction is applied to these points. For the connection points of tower legs which have not changed in position and other points of tower legs that have not suffered from foundation settlement, all translational and rotational freedom degrees of all directions have been fixed. The large deformation option should be opened in ANSYS, and the effect of the large deformation of the tower and wires should be considered.

III. MONITORING LOCATION SELECTION AND ANALYZING SIMULATION RESULTS

According to the results of field survey, the displacement of the tower legs to the original location of the tower has been determined, and the stress and strain distribution of the tower structure has been simulated. By further increasing the displacement value of tower leg nodes, tower under the foundation settlement condition that may occur in the future is simulated so as to determine the strain monitoring position of tower and make a rough assessment of the strain change margin of measuring points according to the simulation results under current working condition and results under the possible working condition in the future.

A. CURRENT SIMULATION RESULTS

In order to determine the freedom constraint of nodes of each tower leg in the simulation process, it is necessary to know the deviation of each tower leg position relative to the original location of each tower leg. According to the results of field survey by geologists, displacement changes of each tower leg are shown in Fig. 4.

As shown in Fig.4, the square patterns of the blue lines represent the original position of the connection point between
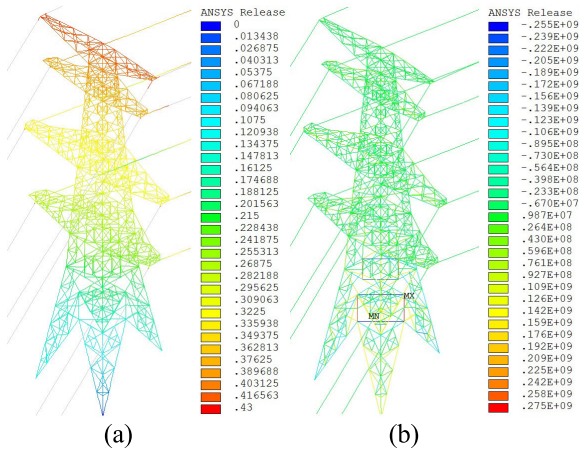
FIGURE 5. Results of the tower-line system simulation. (a) Displacement nephogram of tower 18# nodes, (b) Stress nephogram of tower 18# nodes.

TABLE 1. Stress of arched steels on the first transverse plane.

Element number	1507	1508	1567	1568
Stress/MPa	-254.75	-255.15	-254.20	-249.48

the four tower legs and the ground, and the four tower legs form a square. The square patterns of dotted red lines represent the position after the settlement of the tower, which has changed into a similar diamond shape. The position of tower leg B has not changed, but the deviation of tower leg A, C and D in the directions of x, y and z has occurred compared with the original position. And x represents the direction perpendicular to the wires, y stands for vertical direction, and z stands for the direction along the wires. So it is obvious that tower leg A and C have been squeezed inward, tower leg B and D have been stretched which caused serious deformation of steel of the tower.

Based on the current tower leg positions change, results of the tower-line system simulation have been shown in Fig. 5. The positions with the largest displacement of the tower element are concentrated at the ground wire support arms and cross arms of the tower, and the tower elements with the max stress are concentrated at the first and second transverse plane of the tower body. It can be seen from Fig.2 that two auxiliary elements located on the first transverse plane of the tower appeared arched upward and obvious bending. To verify the correctness and rationality of the simulation results, the stress values of all the corresponding elements on the two auxiliary elements are shown in Table 1.

As can be seen from the above table, the simulated stress values of the arched elements on the first transverse plane under the current working condition are all around −250 MPa, and the yield strength of the steel is 235MPa, which indicates that these elements have been subjected to large compressive force and yielded. This leads to the arch
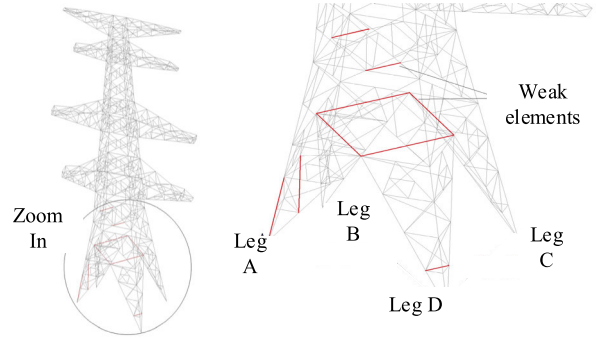

FIGURE 6. Positions of weak components on the tower.

bending and large deformation of the two auxiliary elements, which is consistent with the actual situation. According to the displacement nephogram of tower 18#, the tower has been leaned towards tower 17#, which is consistent with the actual field observation results. This proves the reliability and correctness of the simulation results.

B. LOCATION SELECTION OF MEASURING POINTS
To locate the weak points on the tower accurately, that is, to find the most dangerous and vulnerable elements of the tower, strain measuring devices can be installed on weak elements to monitor the safety status of the tower in real time. By comparing the mechanical simulation results of the tower under the original state and the current working condition, the stress variation of each element of the tower is analyzed, and the weak elements of the tower have been explored. Main and auxiliary elements with maximum stress ratio k below the second transverse plane are selected as shown in Fig.6. The stress ratio k is calculated as follows:

$$k = \frac{\sigma}{[\sigma]} \qquad (3)$$

where σ is simulated stress of elements, $[\sigma]$ is allowable stress of elements.

Elements marked red in Fig.6 have the maximum stress ratio based on simulation results of current working conditions, and they are the most easily yielding elements. They are also the elements with the greatest strain variation under the current load compared with the original state, which shows that strain of these positions are sensitive to the change of land subsidence. Considering that the direction and value of tower foundation settlement will not change greatly in a short time, these elements can be regarded as the weak points of the tower.

Under the current situation, tower leg A and C has been squeezed inward and tower leg B and D has been stretched. As a result, the weak points are mainly concentrated on the first transverse plane and the second transverse plane in the middle of the tower body. The steels on the two transverse planes are auxiliary elements with small yield strength value, which are more prone to yield. This is consistent with the situation observed in the field. At the same time, the foundation
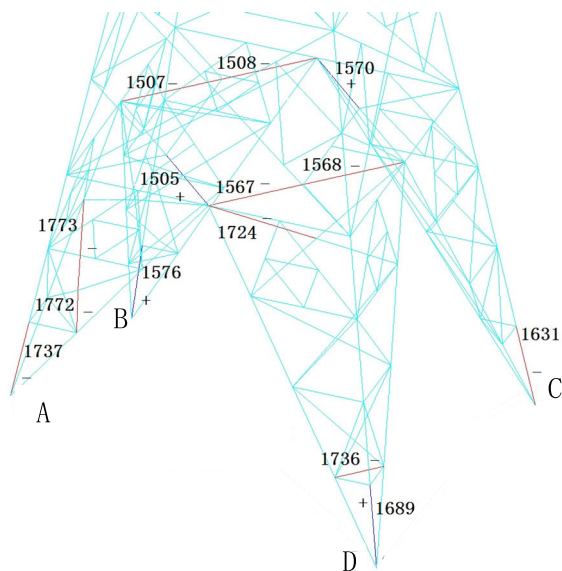
FIGURE 7. Strain monitoring location of weak components.

TABLE 2. Results of monitoring point stress under different working conditions.

No.	Element number	Yield strength /MPa	Stress under condition 1/MPa	Stress under condition 2/MPa	Stress under condition 3/MPa
1	1631	345	23.44	-80.84	-172.96
2	1689	345	42.96	111.44	197.33
3	1737	345	-78.62	-177.94	-277.96
4	1576	345	-70.59	39.69	131.98
5	1736	235	-15.57	-186.44	-277.97
6	1724	235	-1.26	-141.68	-210.83
7	1507	235	-2.22	-254.75	-310.87
8	1568	235	0.28	-249.48	-317.91
9	1505	235	5.15	274.89	369.45
10	1570	235	-2.64	266.58	364.87
11	1508	235	0.97	-255.15	-319.33
12	1567	235	-2.85	-254.20	-316.85
13	1772	235	-2.69	-234.65	-272.91
14	1773	235	-2.98	-222.45	-252.43

settlement causes the tower legs to be compressed or stretched seriously, so some weak points are concentrated in the tower legs, as is shown in the Fig.6.

According to the above mentioned week element positions of tower #18 in Fig.6, considering the convenience of actual implementation, personnel safety, equipment limitations and other factors, 14 elements on or below the first transverse plane have been selected for strain monitoring. The specific location of measurement points is shown in Fig. 7, the positive sign means the element is under tension, while the negative value means the steel structure is under compression.

C. STRESS ANALYSIS OF MEASURING ELEMENTS

By applying displacement constraints of different values to the connecting points of tower legs, mechanical simulation calculation of the tower-line system has been carried out under the following designed three working conditions.

Condition 1: when the tower is completed, which means that there is no foundation settlement or location change of the tower leg under this condition.

Condition 2: Current actual condition of the tower-line system.

Condition 3: The hypothetical working condition when the tower collapses in the future.

Based on the variation of strain and stress at each measuring element under three working conditions, the influence of tower foundation further settlement on stress of elements has been analyzed, and the allowable strain variation margin of measuring elements has been roughly evaluated.

At present, many experts have studied the failure of tower structure system. The transmission tower is a kind of statically indeterminate structure system with many redundant degrees, consisting of many steel elements. The failure of a single tower component may not lead to the failure of the

entire tower system, but when the failure of the corresponding components reaches a certain degree, the tower will be destroyed or even collapsed. Refer to relevant literature and procedures, it is considered that when the main elements yield, horizontal displacement of nodes are too large or the calculated matrix stiffness is singular [18]–[22], specifically, when the stress ratio k of main elements exceeds 1 and that of some auxiliary elements exceeds 1.25 as the settlement of tower foundation increases, the tower is considered to be dangerous and then condition 3 or above can be determined.

Stress changes of each measuring elements under three working conditions are shown in Table 2.

In Table 2, when the tower is completed, there is no foundation settlement or location change of the tower leg, and the elements of the tower 18# bear very little. The maximum stress of the elements at the tower leg (measuring points 1-4) are less than 80MPa, and the stress of the auxiliary elements at the first transverse plane (measuring points 7-12) is almost 0. But with the settlement of the foundation, the stress of the elements at all measuring points increased obviously under condition 2. Auxiliary elements at the first transverse plane exceeded the yield strength, which is consistent with current reality. The main elements at the tower leg A will reach 277.96MPa under condition 3. At this time, the stress of auxiliary elements at measuring points 7~10 and points 11, 12 of the first transverse plane has exceeded 300MPa. Almost auxiliary elements corresponding to all measuring points yields completely, the tower has a high probability of mechanical failure under condition 3.

The strain changes of each measuring element under three working conditions are shown in Table 3.

In Table 3, with the foundation settlement becoming more and more serious, the strain value of steel elements at each

**TABLE 3.** Results of monitoring point strain under different working conditions.

No.	Element number	Strain under condition 1/$\mu\varepsilon$	Strain under condition 2/$\mu\varepsilon$	Strain under condition 3/$\mu\varepsilon$
1	1631	116.13	-454.01	-1057.40
2	1689	215.71	643.16	1218.97
3	1737	-421.32	-1086.07	-1919.55
4	1576	-371.26	224.34	821.11
5	1736	-77.44	-978.46	-1666.91
6	1724	-6.13	-740.93	-1381.88
7	1507	-10.82	-4194.54	-6802.04
8	1568	1.35	-4042.04	-7161.78
9	1505	4.74	-4199.08	-7260.33
10	1570	-13.88	-4187.11	-7091.41
11	1508	25.40	4941.96	15452.76
12	1567	-13.00	4647.07	14213.61
13	1772	-13.3	-1374.00	-4765.42
14	1773	-14.57	-1169.37	-4130.79

FIGURE 8. Site construction photos. (a) The workers installed sensors, (b) Installed sensor on first transverse plane of tower 18#.

measuring point also increases significantly. From the current working condition 2 to the hypothetical working condition 3 when the tower collapses in the future, the main elements of tower legs have a variation of more than $600\mu\varepsilon$. Other auxiliary measuring elements have a variation of more than $1000\mu\varepsilon$. Parts of the auxiliary elements have yielded and the steel has entered the plastic deformation stage under the current working condition. Therefore, compared with the main elements that have not yielded, strain of the auxiliary elements has changed more when they bear the same stress. By monitoring the strain changes of the 14 measuring points, we can analyze the trend of the strain curve and strain value of elements at each measuring point in real-time. Compared with the finite element simulation results, then warning of the failure of the tower can be sounded in short time. If strain prediction results of measuring points 1~4 exceeds $600\mu\varepsilon$ or strain prediction results of measuring points 5~14 exceeds $1000\mu\varepsilon$, measures must be taken to deal with the possible collapse of the tower, such as activating backup lines and evacuating nearby residents which is beneficial to reduce the economic loss or other hazards caused by the tower failure.

IV. REAL-TIME STRAIN MONITORING

Resistance strain slices are installed on the elements of the 14 measurement points, and their measurement signals have been transmitted to the strain device through the signal line to the computer acquisition system. As a result, real-time strain monitoring data can be obtained from the monitoring system.

The strain monitoring system used in this paper is mainly based on resistance strain sensor. Strain rosette consisted of biaxial BX120-3BA has been glued to the surface of the elements being tested. The strain gauge consists of two resistors perpendicular to each other. When the stress of the
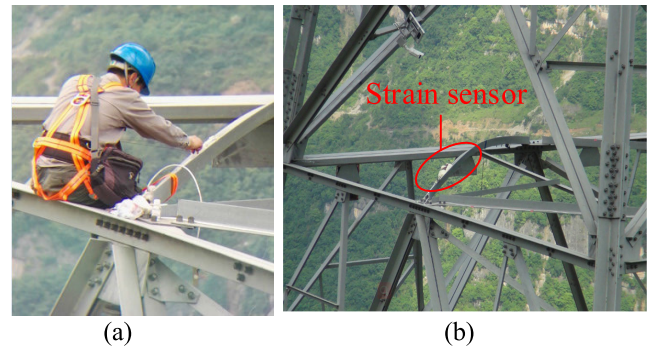
measured objects changes, the resistance strain slice will be stretched or compressed, causing the current change of the resistance sheet. The variation of strain can be calculated by measuring the changed current. Half-bridge circuit is adopted for strain measurement to eliminate the effect of temperature on measurement results. The strain gage device is enclosed in a shielded metal box with grounding well and high quality shielded wire has been used to reduce the electromagnetic interference.

Strain device used in the strain monitoring system is uT7116Y high speed static strain gauge. The strain test device is a static resistance strain gauge with ARM7 CPU and touch screen function. It can communicate with computer USB directly through uT71USB485 module. The measurement range was $0 \sim 30000\mu\varepsilon$ and the measurement error was only $\pm0.01\%FS\pm0.5\mu\varepsilon$.

The key of strain measurement is that the resistance strain slice is in good contact with the measured object. However, due to the particularity of tower, it is difficult to paste strain slice directly on the steels of tower and carry out relevant waterproofing treatment, preventing obtaining of satisfactory measurement data. Therefore, the strain slice is generally packaged in a metal box. By sticking the box on the steel when measuring, it is not only convenient for field installation, but also improves its waterproof performance. After installation, it is necessary to apply waterproof and moisture-proof silicone rubber 703 on the entire surface of the box, especially around the edge of the box. When the silicone rubber solidifies, the expanded adhesive with insulation and fixing effect will smear on the whole surface to reduce the measurement error. Photos of actual construction site are shown in Fig. 8.

The sampling frequency was set at 0.2 Hz, and the above strain monitoring system was used for real-time monitoring of steel strain at the 14 measuring points of the tower 18# before the new transmission tower is built. The monitoring device was in normal operation at the site for about a month. The curves of monitoring strain of part elements over time in a certain period are shown in Fig. 9.

According to Fig. 9, the strain curves of elements at the measurement point fluctuate within a certain range, and the
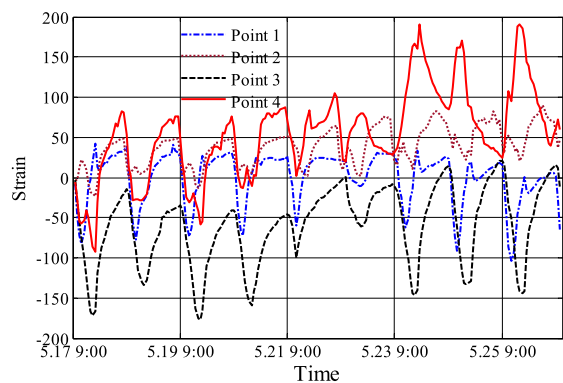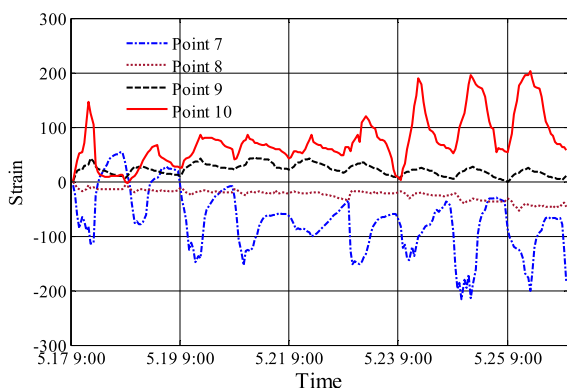
FIGURE 9. Strain curves of the monitoring steels. (a) Curve of strain change at the elements of the tower legs, (b) Curve of strain change at the first transverse partition.

fluctuation period lasts approximately 24h, which is mainly affected by the temperature variations between day and night and the environmental change. The strain variation curves of the four monitoring points (monitoring points 1-4) at the tower legs fluctuated stably with time, and the strain fluctuation range was less than $250\mu\varepsilon$. The fluctuation range of strain curves of inclined elements on the first transverse plane fluctuates was about -200~200$\mu\varepsilon$, and the fluctuation trend of compression components (monitoring points 7 and 8) is completely opposite to that of tensile components (monitoring points 9 and 10), which confirms the reliability of the monitoring results.

V. STRAIN FORECASTING USING ARIMA MODEL

Time series analysis and forecasting is an active research area. Several research studies on time series forecasting have been proposed with various methods over the years. And it has been widely used in many fields such as weather, stock, power load forecasting, voice recognition and so on [23]–[30]. Up to now, time series forecasting models can be divided into three directions: traditional statistical model, artificial intelligence model and hybrid model.

At present, few time series prediction methods are used in the early failure warning of transmission lines. The following conditions must be met for the prediction of time

TABLE 4. ADF test results of original strain series.

No.	Lags	Value of 'p'
1	14	0.3194
2	12	0.3863
7	12	0.2530

series: first, the past, present and future objective conditions of the prediction variables remain basically unchanged, and the laws of historical data interpretation can be extended to the future; second, the development process of predictive variables is gradual, rather than jumping or mutation. In this paper, the strain variation of transmission tower elements is related to many factors, such as temperature, humidity, wind, land subsidence, etc. These factors have certain rules in short term, and settlement of tower foundation caused by land subsidence is gradually varied and slow usually. So the matching prediction model can be used for tower elements strain prediction. Through the prediction, the strain value of key elements after a few hours can be known in advance, so as to make early warning of the safety status of the tower in time, and the staff has plenty of time to respond to what is about to happen.

A. TIME SERIES ANALYSIS

1) STATIONARITY OF A TIME SERIES

After obtaining the tower strain time series, it is necessary to ensure that the series is stationary or not. If the series is non-stationary, then the series has to be differentiated so as to make it stationary, otherwise the time series cannot be predicted. If a time series is stationary, which means that it is only related with the variable time interval and has nothing to do with the starting and ending point. It shows that the mean value and covariance of the series in a fixed period of time do not change with time. There are certain tests that assist in checking whether the series is stationary, such as "W-D test", "L-jung-Box test", "t-statistic test", the "Kwiatkowski-Phillips-Schmidt-Shin (KPSS) test" and "Augmented Dickey-Fuller unit root test (ADF test)" [27], [28].

The strain series have been checked by the ADF test. It is a standard statistical test for stationarity. If the value of 'p' is less than 0.05 or 5% for a time series, then the series is supposed to be stationary. Take the strain series of measurement points 1, 2 and 7 as an example, the test results have been shown in Table 4.

The smaller the value of 'p' is, the more stable the time series is. From Table 3, all the original series test results are greater than 0.05, which shows that the strain series is non- stationary. So it needs to be corrected by means of differentiating [27], [28]. An easy way is to compute the differences between consecutive observations of the series.

2) WHITE NOISE TEST

When forecasting a time series, it is necessary to ensure that the time series has certain relevance. If the time series has no correlation, then it is impossible to analyze the change trend of the series. Therefore, the historical data of the series in the past cannot provide valuable information to deduce the development trend of the future. Such series without regularity belong to white noise series.

The L-jung-box test was used to test if the original strain series belongs to white noise series. The original hypothesis holds that there is no correlation between the time series data, and the series is white noise series. Take the strain series of measurement points 1, 2 and 7 as an example, the test results are all approximately equal to 0 and far less than 0.05. So the null hypothesis to be white noise has been rejected, which shows that the strain time series data passes the white noise test, and it can be used for prediction and simulation of meteorological processes.

3) SERIES DECOMPOSITION

The decomposition of the time series data into its essential constituents is needed to be done. Decomposing the time series data helps in revealing a lot of hidden patterns inside the time series. Generally speaking, a time series is composed of the following components: Trend component (T), cyclic component (C), seasonal component (S) and irregular component (I). The trend component is the general trend of change caused by some fundamental factor over a long period of time. The seasonal component represents the regular periodic fluctuations influenced by seasonal factors and repeat at regular periodic intervals like weekly, fortnightly or monthly. The cyclic component is present in a time series when the time series displays a rise and fall of irregular time period. The irregular component is a random fluctuation excluding the other three parts of the series. Actual observation series data $Y(t)$ is made up of these four parts, the composing form is additive model or multiplication model usually [29]. The additive model is shown as below:

$$Y(t) = T(t) + C(t) + S(t) + I(t) \qquad (4)$$

The strain series have been decomposed into the trend component (T), seasonal component (S) and the residual component (R) by using 'Statsmodels' tool package in Python based on the above additive model. Take the strain series of measurement points 1 as an example, the result after decomposition has been shown in Fig. 10.

B. STRAIN FORECASTING MODEL

The autoregressive integrated moving average (ARIMA) model is widely regarded as the most efficient statistical forecasting technique and it has been used in many fields. It is a generalization of the autoregressive moving average (ARMA) model.

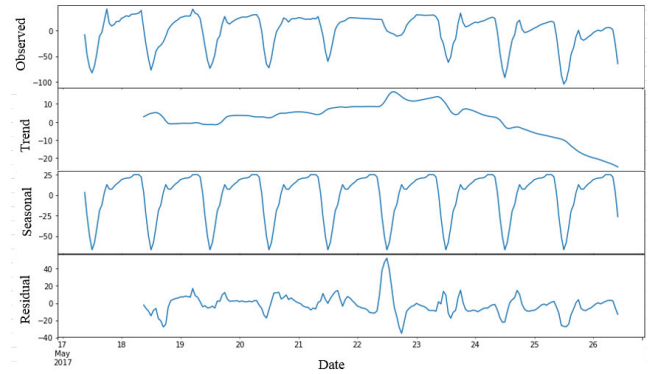The "Autoregressive" (AR) along with "moving average" (MA) models have been combined to get a new time series

FIGURE 10. Decomposition of monitoring strain time-series data.

models referred as "ARMA models". The general notation for the "ARMA (p, q) model" is as:

$$y_t = (\phi_0 + \phi_1 y_{t-1} + \phi_2 y_{t-2} + \ldots + \phi_p y_{t-p})$$
$$+ (\varepsilon_t + \theta_1 \varepsilon_{t-1} + \theta_2 \varepsilon_{t-2} + \ldots + \theta_q \varepsilon_{t-q}) \qquad (5)$$

where $\phi_p \neq 0$, $\theta_q \neq 0$, $E(\varepsilon_t) = 0$, $\text{Var}(\varepsilon_t) = \delta^2$, $E(\varepsilon_t, \varepsilon_s) = 0$, $\forall s \neq t$. In the above given equation, ϕ_p and θ_q are the parameter of AR model and MA model.

The name of ARIMA model "ARIMA $(AR+I+MA)$" stands for "Auto-regressive Integrated Moving Average". This model is also often called by the famous "Box-Jenkins model". The ARMA model is only suitable for the stationary time series data but usually most time series shows non-stationary properties. This model claims that a non-stationary series could be changed to stationary by means of differentiating it. The general notation for the "ARIMA (p, d, q) model" is as:

$$\nabla y_t = (\phi_0 + \phi_1 \nabla y_{t-1} + \phi_2 \nabla y_{t-2} + \ldots + \phi_p \nabla y_{t-p})$$
$$+ (\varepsilon_t + \theta_1 \varepsilon_{t-1} + \theta_2 \varepsilon_{t-2} + \ldots + \theta_q \varepsilon_{t-q}) \qquad (6)$$

where ∇y_t is "differentiating time series" that have been differentiating once or more, d is the number of the differentiating. Parameter p and q represent the same meaning as ARMA model, that is, p is the order of auto-regressive part and q is the order of the moving average part of the whole ARIMA predict model [28].

The strain time series has been decomposed to T, S and R before, now it is necessary to establish the ARIMA prediction models for the trend component and the residual component respectively since the seasonal component is fixed. After getting the predict value of T and R, the strain time series forecasting results can be calculated as follow:

$$\hat{y}_t = \hat{T}_t + \hat{R}_t + S_t \qquad (7)$$

where $\hat{y}_t$ is the forecasting result of the strain series, $\hat{T}_t$ is the forecasting result of the trend component, $\hat{R}_t$ is the forecasting result of the residual component. The method eliminates the periodic component of the series data and reduces the nonlinearity of the data, which is helpful to improve the accuracy and rationality of the prediction results.
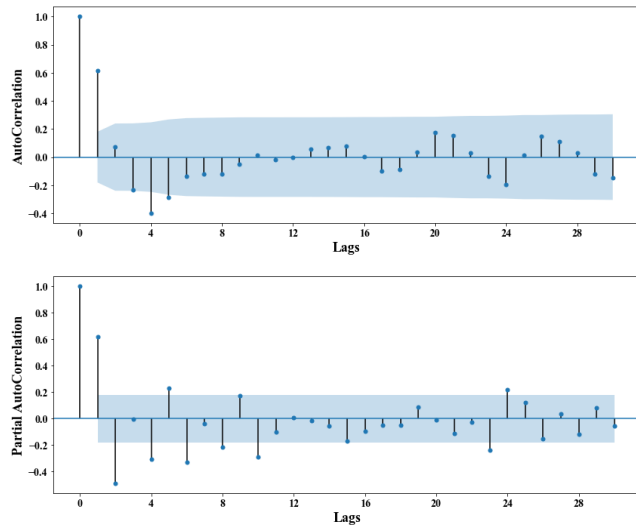
FIGURE 11. "ACF and PACF" plots for series 'T'.

FIGURE 12. Strain rolling prediction results of monitoring point 1.

FIGURE 13. Strain rolling prediction results of monitoring point 7.

Take the strain series of measurement points 1 as an example, data from May 17 9:00 to May 22 9:00 has been used as training samples. The trend component ARIMA prediction model has been established firstly. After twice differentiating, series 'T' can be transformed into a stationary time series. The next thing we need to do is to plot the "ACF and PACF" plots meant for time series data. From the "ACF and PACF" plots, the approximate value range of p and q can be preliminarily determined. The ACF and PACF plots of differenced series 'T' have been given as below in Fig. 11.

Fig. 11 shows that p is within 8 and q is within 6. Then the information criterion function has been used to determine the order of the model. Through cyclic calculation of the model AIC, BIC and HQIC value, the lowest value of the three information criterion value suggest the best model for prediction. In this case it is (2, 2, 5). Thus we have got the best suited parameters (p, d, q) for the model and we can use the ARIMA model to obtain the forecast result of series 'T'.

After the prediction is completed, it is needed to check the prediction model. The usual practice is to use the L-Jung-Box test for the validation of the predicted series to check if the residuals are random. The p value obtained in the test is 0.7076, much higher than 0.05. Therefore, the null hypothesis is accepted and the residual time series is considered as white noise series, and there is no correlation between the sequences. Or we can say the ARIMA prediction model has completely extracted the valid information of the original time series and it will get a satisfying result.

Next the series 'R' has been forecasted and the establishment process of prediction model is consistent with the above series 'T'. Its best suited parameters (p, d, q) is (1, 0, 3). The prediction results of strain time series can be obtained by adding prediction results of series 'T', 'R' and seasonal components 'S'.
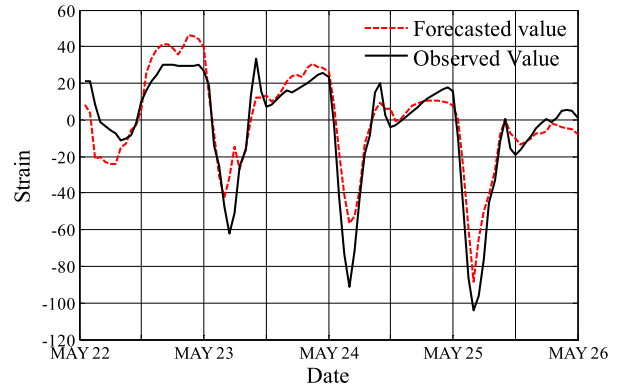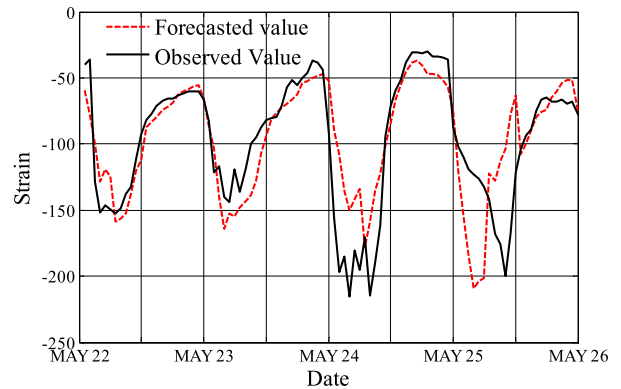
C. RESULTS

After the exploration of the prediction model, this paper takes 6 hours as the prediction period and makes rolling prediction of strain time series of each monitoring point based on the above-mentioned ARIMA prediction model. That is, the most recent 120h monitoring data is used to predict the next 6 hours, and then the most recent 120h monitoring data is used to predict the next 6 hours until 9:00 am on May 26. Taking monitoring point 1 as an example, the rolling prediction results and actual results are shown in Fig. 12.

As can be seen from the Fig. 12, a rolling prediction model of strain time series is established based on the above ARIMA prediction model with a fixed interval of 6h, and the prediction results can reflect the change trend of the original measured data well. Most of the time the forecast error is within $20\mu\varepsilon$. The prediction results are accurate. To prove that the prediction was not accidental, take monitoring point 7 as an example, its rolling prediction results and actual results are shown in Fig. 13.

Strain time series prediction results of measuring point 7 are almost consistent with the actual observed values. Most of the time the forecast error is within $50\mu\varepsilon$. There are several methods to evaluate a time series prediction model's accuracy. Following three different evaluation statistics have been calculated to examine the forecasting accuracy: the mean absolute error (MAE), the root mean square error (RMSE)

TABLE 5. Evaluation statistics of ARIMA model.

No.	MAE	RMSE	MSPE
1	9.63	12.84	28.12%
7	22.41	32.53	2.99%

and the mean square percent error (MSPE) [30]. They are expressed in the following:

$$MAE = \frac{1}{n} \sum_{t=1}^{n} |y_t - \hat{y}_t|$$

$$RMSE = \sqrt{\frac{1}{n} \sum_{t=1}^{n} (y_t - \hat{y}_t)^2}$$

$$MSPE = \frac{1}{n} \sqrt{\sum_{t=1}^{n} \left(\frac{y_t - \hat{y}_t}{y_t}\right)^2} \times 100\%$$

where y_t and $\hat{y}_t$ are the actual and predicted values respectively, and n is the total number of predictions.

Evaluation statistics results of the three error indicators for ARIMA prediction model of measuring point 1 and 7 have been shown in Table 5.

Through the prediction, the strain value of key elements after a few hours can be known in advance. Combining the prediction results with the above finite element simulation results in Part III, we can make early warning of the safety status of the tower in time and take corresponding measures. The prediction model has a certain ability of resisting external interference. Even if there is a misjudgment caused by random excitation, such as falling rocks, the signal will be corrected in the short term since the prediction is a constant rolling process. Therefore, the early warning results of the tower are reliable. By using this method, we successfully monitored the strain of the tower 18# within a month until it was safely dismantled.

VI. CONCLUSION

This paper puts forward a short-term failure warning method for transmission tower under land subsidence condition based on the finite element simulation, strain monitoring and ARIMA time series forecast model. This method has been successfully applied to an actual 500kV transmission line emergency treatment under land subsidence condition.

A precise tower-line system model based on finite element method has been established. By simulating the stress distribution of the tower under actual foundation settlement condition, the weak components of the settlement tower have been located. Combined with the finite element simulation results in various conditions, the reliability of simulation results is verified, and the strain variation range of the corresponding measuring point is obtained, which provides a basis for judging the safety status of the tower.

Strain time series have been obtained by installing resistance-based strain monitoring device on the tower.

By building ARIMA model of its trend component and seasonal component respectively, the rolling strain series forecasting results have been obtained. Strain time series prediction results are almost consistent with the actual observed values, and most of the time the forecast error is within $50\mu\varepsilon$.

In the future, a better strain monitoring method for transmission towers is needed to be researched since the resistance strain sensor is not suitable for long-term on-line monitoring. Some other prediction models, such as LSTM, can be studied for the strain time series forecasting to obtain a longer and more accurate prediction result, which can provide more accurate suggestions for the early warning of tower failure.

REFERENCES

[1] L. I. Qing-Feng, Z. Fan, Q. Wu, J. Gao, Z. Y. Su, and W. J. Zhou, "Investigation of ice-covered transmission lines and analysis on transmission line failures caused by ice-coating in China," *Power Syst. Technol.*, vol. 32, no. 9, pp. 33–36, 2008.

[2] F. Yang, J. Yang, J. Han, and Z. Zhang, "Study on the limited values of foundation deformation for a typical UHV transmission tower," *IEEE Trans. Power Del.*, vol. 25, no. 4, pp. 2752–2758, Oct. 2010.

[3] X. Huang, L. Zhao, Z. Chen, and C. Liu, "An online monitoring technology of tower foundation deformation of transmission lines," *Struct. Health Monitor.*, vol. 18, no. 3, pp. 949–962, May 2019.

[4] S. Gu, J. Wang, M. Wu, J. Guo, C. Zhao, and J. Li, "Study on lightning risk assessment and early warning for UHV DC transmission channel," *High Voltage*, vol. 4, no. 2, pp. 144–150, Apr. 2019.

[5] F. Al-Bermani and S. Kitipornchai, "Nonlinear analysis of transmission towers," *Eng. Struct.*, vol. 14, no. 3, pp. 139–151, Jan. 1992.

[6] N. Prasad Rao, G. M. Samuel Knight, S. Seetharaman, N. Lakshmanan, and N. R. Iyer, "Failure analysis of transmission line towers," *J. Perform. Constructed Facilities*, vol. 25, no. 3, pp. 231–240, Jun. 2011.

[7] Z. Y. Du, Y. Zhang, and R. Jiangjun, "Failure analysis of 500kV iced overhead transmission line by finite element method," *High Voltage Eng.*, vol. 38, no. 9, pp. 2430–2436, Sep. 2012.

[8] C. G. Yao, F. Mao, D. Xu, X. Liu, Z. Zhou, and Y.-J. Cui, "Prediction method for accidents of ice covered tower-line system using the mechanical feature of key components," *High Voltage Eng.*, vol. 37, no. 2, pp. 476–483, Feb. 2011.

[9] X.-X. Cheng, Y. Peng, Z. A. Khan, and J. Dong, "Beam-end stiffness identification for a structural health monitoring-oriented finite-element transmission tower model using effective optimization techniques," *Adv. Struct. Eng.*, vol. 22, no. 2, pp. 364–383, Jan. 2019.

[10] Y.-Z. Ju, Q.-L. Xue, and H. Li, "Failure analysis of transmission tower under the effect of ice-covered power transmission line," in *Proc. 1st Int. Conf. Inf. Sci. Eng.*, Jun. 2009, pp. 4301–4304.

[11] S. Malhara and V. Vittal, "Mechanical state estimation of overhead transmission lines using tilt sensors," *IEEE Trans. Power Syst.*, vol. 25, no. 3, pp. 1282–1290, Aug. 2010.

[12] L. P. Li, L. Y. Shan, M. Y. Zhang, and Y. Wang, "Monitoring to the transmission towers' inclination on-line system based on GPRS," in *Proc. 2nd Int. Conf. Artif. Intell., Manage. Sci. Electron. Commerce (AIMSEC)*, Aug. 2010, pp. 4080–4083.

[13] Y. Liu, Y. Hu, L. N. Wang, K. Liu, J. Hu, T. Liu, and B. Xiao, "Surveillance for 1000 kV transmission tower deformation using high-resolution SAR satellite," *High Voltage Eng.*, vol. 35, no. 9, pp. 2076–2079, Sep. 2009.

[14] X. Huang, M. Liao, G. Xu, Y. Zhu, and L. Zhao, "Stress monitoring method applying FBG sensor for transmission line towers," *Electr. Power Autom. Equip.*, vol. 36, no. 4, pp. 68–72, Apr. 2016.

[15] Y. Zhang and X. Song, "Load prediction of space deployable structure based on FBG and LSTM," *IEEE Access*, vol. 7, pp. 13715–13722, 2019.

[16] D. F. Ma, H. S. Cai, and L. B. Zhang, "Stress monitoring research in dancing condition of transmission tower based on FBG sensors," in *Proc. Int. Conf. Renew. Energy Environ. Technol.*, Sep. 2013, pp. 2249–2253.

[17] M. Li and Y. J. Xu, "Fiber Bragg grating sensor technology for status monitoring of overhead transmission line," *Telecommun. Electr. Power Syst.*, vol. 33, no. 11, pp. 59–64, Nov. 2012.

[18] D. Dong, J. Hou, L. Xiao, X. An, and M. Li, "Development of calculation program for identifying main failure modes of transmission tower system," *Eng. Mech.*, vol. 30, no. 8, pp. 180–185, Aug. 2013.

[19] X. Gao and S. L. Li, "Dominant failure modes identification and structural system reliability analysis for a long-span arch bridge," *Struct. Eng. Mech.*, vol. 63, no. 6, pp. 799–808, Sep. 2017.

[20] F. Han, "Study on reliability analysis of UHV transmission tower-line system with wind action," Ph.D. dissertation, College Civil Eng., Chongqing Univ., Chongqing, China, 2012.

[21] J. J. Feng, "The reliability of transmission tower under the environmental load," M.S. thesis, School Hydraulic Eng., Dalian Univ. Technol., Dalian, China, 2012.

[22] H. R. Zhang, "Research on failure warning technology of strain tower under Icing condition," *Southern Power Syst. Technol.*, vol. 12, no. 1, pp. 33–40, Jan. 2018.

[23] M. Zhou, Z. Yan, Y. Ni, G. Li, and Y. Nie, "Electricity price forecasting with confidence-interval estimation through an extended ARIMA approach," *IEE Proc.-Gener. Transmiss. Distrib.*, vol. 153, no. 2, pp. 187–195, Mar. 2006.

[24] K. Yunus, T. Thiringer, and P. Chen, "ARIMA-based frequency-decomposed modeling of wind speed time series," *IEEE Trans. Power Syst.*, vol. 31, no. 4, pp. 2546–2556, Jul. 2016.

[25] M. Dorraki, A. Fouladzadeh, S. J. Salamon, A. Allison, B. J. Coventry, and D. Abbott, "Can C-reactive protein (CRP) time series forecasting be achieved via deep learning?" *IEEE Access*, vol. 7, pp. 59311–59320, 2019.

[26] V. Tsioumas, S. Papadimitriou, Y. Smirlis, and S. Z. Zahran, "A novel approach to forecasting the bulk freight market," *Asian J. Shipping Logistics*, vol. 33, no. 1, pp. 33–41, Mar. 2017.

[27] K. V. N. Murthy, R. Saravana, and K. V. Kumar, "Modeling and forecasting rainfall patterns of southwest monsoons in North–East India as a SARIMA process," *Meteorol. Atmos. Phys.*, vol. 130, no. 1, pp. 99–106, Jan. 2018.

[28] S. M. Idrees, M. A. Alam, and P. Agarwal, "A prediction approach for stock market volatility based on time series data," *IEEE Access*, vol. 7, pp. 17287–17298, 2019.

[29] D. Gerbing, *Time Series Components*. Portland, OR, USA: Portland State Univ., 2016, p. 9.

[30] S. Liu, S. Gu, and T. Bao, "An automatic forecasting method for time series," *Chin. J. Electron.*, vol. 26, no. 3, pp. 445–452, May 2017.
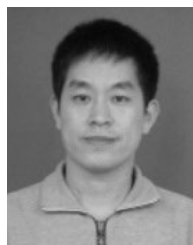
ZHIYE DU (Member, IEEE) was born in Xuchang, Henan, China, in 1974. He received the M.S. degree and the Ph.D. degree in electrical engineering from Wuhan University, Wuhan, China, in 2004 and 2007, respectively. He is currently a Professor with the School of Electrical Engineering and Automation, Wuhan University. His major interests are high-voltage technology, numerical analysis of electro-magnetic problems, and nondestructive testing.

WENFENG ZHOU was born in Jiujiang, Jiangxi, China, in 1995. He received the B.S. degree in electrical engineering and automation from the School of Electrical Engineering and Automation, Wuhan University, Wuhan, China, in 2017, where he is currently pursuing the master's degree in electrical engineering. His research interests include transmission line risk assessment, high voltage, and insulation technology.

GUANNAN LI was born in Sichuan, China, in 1994. He received the B.S. degree in electrical engineering and automation from the School of Electrical Engineering and Automation, Wuhan University, Wuhan, China, in 2017, where he is currently pursuing the master's degree in electrical engineering. His research interests include the numerical calculation of electromagnetic field, high voltage, and insulation technology.

LI ZHANG was born in Hubei, China, in 1994. He received the B.S. degree in electrical engineering and automation from the School of Electrical Engineering and Automation, Wuhan University, Wuhan, China, in 2015, where he is currently pursuing the Ph.D. degree in electrical engineering. His research interests include transmission line risk assessment, condition monitoring of transmission tower, high voltage, and insulation technology.

JIANGJUN RUAN (Member, IEEE) was born in Zhejiang, China, in 1968. He received the B.S. and Ph.D. degrees in electric machine engineering from the Huazhong University of Science and Technology, Wuhan, China, in 1990 and 1995, respectively. He was a Postdoctoral Researcher with the Wuhan University of Hydraulic and Electric Engineering, Wuhan, in 1998. He is currently a Professor with the School of Electrical Engineering and Automation, Wuhan University. His research interests include electromagnetic field numerical simulation, high voltage, and insulation technology.
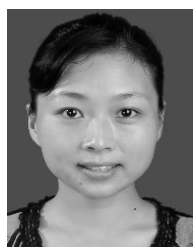
YAN GAN was born in Yingcheng, Hubei, China, in 1976. She received the M.S. and Ph.D. degrees in electrical engineering from Wuhan University, Wuhan, China, in 2004 and 2007, respectively. She is currently a Professor-Level Senior Engineer with Central China Branch of the State Grid Corporation. Her major field of interest is high-voltage technology and numerical analysis of electromagnetic problems in engineering.

• • •